LA-UR -92-367

LA-UR--92-367 M--1

DE92 008445

Los Alamos National Laboratory is operated by the University of California for the United States Department of Energy under contract W-7405-ENG-36

TITLE: **EXTENDING NEC TO MODEL WIRE OBJECTS IN INFINITE CHIRAL MEDIA**

AUTHOR(S): G.J. Burke, LLNL
E.K. Miller, MEE-3
A.K. Bhattacharyya, NMSU

SUBMITTED TO: ACES
Monterey, CA
March 17, 1992

EXTENDING NEC TO MODEL WIRE OBJECTS IN INFINITE CHIRAL MEDIA

G. J. Burke, L-156
Lawrence Livermore National Laboratory
PO Box 5504, Livermore, CA 94550

E. K. Miller, MS J-580
Los Alamos National Laboratory
PO Box 1663, Los Alamos, NM 87545

A. K. Bhattacharyya
New Mexico State University, Physical Science Laboratory
PO Box 30002, Las Cruces, NM 88003

Abstract
The development of a moment-method model for wire objects in an infinite chiral medium is described. In this work, the Numerical Electromagnetics Code (NEC) was extended by including a new integral-equation kernel obtained from the dyadic Green's function for an infinite chiral medium. The NEC moment-method treatment using point matching and a three-term sinusoidal current expansion was adapted to the case of a chiral medium. Examples of current distributions and radiation patterns for simple antennas are presented, and the validation of the code is discussed.

Introduction
Interest has been growing recently in the uses and behavior of chiral media in electromagnetic applications. Chiral media can be thought of as ordinary media in which are distributed small helices of either right-hand or left-hand rotation. As a result, waves with linear polarization cannot propagate, and waves with right- or left-hand circular polarization propagate differently in the medium. The pertinent canonical problems were formulated sometime ago [Bassiri, Engheta and Papas (1986), Lakhtakia, Varadan and Varadan (1986)], e.g. point-source radiation, wave propagation and scattering. Interest is growing in more practical problems due to the advent of chiral composites and research is being conducted for chirality might be exploited in electromagnetic design. Research in chiral media has made continued progress in developing analytical tools for understanding fundamental electromagnetic behavior [e.g., Lakhtakia, Varadan and Varadan (1989), Lakhtakia (1990), Lakhtakia, Varadan and Varadan (1990), Uslenghi (1990), Lakhtakia, (1991), Engheta, Pelet and Li (1991)] but the results thereof remain of somewhat limited applicability. In order to analyze the behavior of complex radiators in chiral media it is necessary to resort to numerical techniques such as the integral-equation models (e.g., like NEC) that have become routine tools for many years in analyzing radiation and scattering in achiral media.

In this paper, extension of NEC [Burke and Poggio (1981)] to model arbitrary wire objects in chiral media is briefly summarized, continuing work described elsewhere [Bhattacharyya (1990), Bhattacharyya, Burke and Miller (1992a), (1992b)]. First, a new kernel is implemented in the Electric-Field Integral Equation (EFIE) for thin wires, starting from the dyadic Green's function for a chiral medium. Then the solution of this equation using point-matching and a three-term sinusoidal current expansion is developed. Finally, examples are shown of the solutions obtained for typical dipole and loop antennas operating in chiral media to demonstrate the effects of chirality on current distributions and impedance.

Formulation of the EFIE for Chiral Media
The EFIE for chiral media is conveniently formulated by starting with the dyadic Green's function

for an infinite chiral medium, one form of which is given by Bassiri (1990) (dyadic quantities are outlined and vectors are boldface)

$$\boldsymbol{\Gamma}_{\text{chiral}}(\mathbf{r},\mathbf{r}') = a_1\left(\mathbb{I} + \frac{1}{h_1}\mathbb{I}\times\nabla + \frac{1}{h_1^2}\nabla\nabla\right)\frac{e^{-jh_1R}}{4\pi R} + a_2\left(\mathbb{I} - \frac{1}{h_2}\mathbb{I}\times\nabla + \frac{1}{h_2^2}\nabla\nabla\right)\frac{e^{-jh_2R}}{4\pi R} \qquad (1)$$

where

$$a_1 = \frac{h_1^2 - k^2}{h_1^2 - h_2^2},\; a_2 = -\frac{h_2^2 - k^2}{h_1^2 - h_2^2}$$

and h_1 and h_2 are the wavenumbers for right- and left-hand circularly-polarized waves in the medium as given by

$$h_{1,2} = \pm\omega\mu\gamma + \sqrt{(\omega\mu\gamma)^2 + k^2}.$$

The chirality constant γ determines the degree of chirality of the medium, and $k = \omega\sqrt{\mu\varepsilon}$ where μ and ε are the medium permeability and permittivity respectively.

The electric field at a point **r** due to a current distribution **J(r)** is given by

$$\mathbf{E}(\mathbf{r}) = j\omega\mu\int \boldsymbol{\Gamma}(\mathbf{r},\mathbf{r}')\cdot\mathbf{J}(\mathbf{r}')dV'$$

so that an integral equation for the current can be derived in the usual way using the thin-wire approximation. We thus obtain

$$j\omega\mu\int_{C(s)} I(s')\hat{\mathbf{s}}\cdot\boldsymbol{\Gamma}(\mathbf{r},\mathbf{r}_a')\cdot\hat{\mathbf{s}}'ds' = -\hat{\mathbf{s}}\cdot\mathbf{E}^{inc}(\mathbf{r}),\; \mathbf{r}\in C(s) \qquad (2)$$

where $\hat{\mathbf{s}}$ and $\hat{\mathbf{s}}'$ are unti vectors tangent to the wire axis at observation point s and source point s' respectively. By letting **r** represent a point on the wire axis at s while $\mathbf{r}_a'$ is a point on the wire surface at s', the problem of the singularity in the Green's function is avoided for the thin wire. The incident field, $\mathbf{E}^{inc}$, may be an incident wave or a localized field due to a voltage source.

Numerical Solution of the EFIE for Chiral Media

NEC was used as a starting point for developing a code for wires in chiral media, since much of the present code can be used. For modeling wires, NEC employs point matching and a three-term sinusoidal current expansion, which on segment i has the form

$$I_i(s) = A_i + B_i\sin[k_s(s - s_i)] + C_i\cos[k_s(s - s_i)],\; |s - s_i| \le \Delta_i/2 \qquad (3)$$

where Δ_i is the segment length. Continuity conditions are imposed on current and its derivative to obtain basis functions extending over three segments with the shape of a B-spline. For ordinary media, k_s is set equal to the wave number in the medium, but for the chiral medium a different choice is made as indicated below.

Extension of NEC to chiral media is simplified by noting that, expect for the $\omega \mathbf{x} \nabla$ terms, Eq. (1) has the form of the free-space Green's function for two separate wave numbers h_1 and h_2. Hence, much of the existing NEC can be used. However, the fields due to the $\sin(k_s s)$ and $\cos(k_s s)$ terms in Eq. (3) now involve addition integrals that must be evaluated numerically or by series approximation because closed-form expressions are not available. For wavenumber k_1 and using

$$I(s) = I_0 \begin{pmatrix} \sin(k_s s) \\ \cos(k_s s) \end{pmatrix}$$

for the current on a segment extending from $-\delta$ to $+\delta$ on the z axis, the ρ and z components of the electric field are given by

$$E_\rho(\rho,z) = \frac{-j\eta I_0}{4\pi k_1 \rho} \left\{ \begin{pmatrix} \sin k_s z' \\ \cos k_s z' \end{pmatrix} \left[1 - (z-z')^2 \frac{a + jk_1 R}{R^2} \right. \right.$$

$$\left. \left. + k_s \begin{pmatrix} \cos k_s z' \\ -\sin k_s z' \end{pmatrix} (z-z') \frac{e^{-jk_1 R}}{R} \right]_{-\delta}^{\delta} - (k_1^2 - k_s^2) \int_{-\delta}^{\delta} \begin{pmatrix} \sin k_s z' \\ \cos k_s z' \end{pmatrix} (z-z') \frac{e^{-jk_1 R}}{R} dz' \right\} \quad (4)$$

and

$$E_z(\rho,z) = \frac{-j\eta I_0}{4\pi k_1} \left\{ \begin{pmatrix} \sin k_s z' \\ \cos k_s z' \end{pmatrix} \left[(z-z')^2 \frac{1 + jk_1 R}{R^2} - k_s \begin{pmatrix} \cos k_s z' \\ -\sin k_s z' \end{pmatrix} \right] \frac{e^{-jk_1 R}}{R} \right]_{-\delta}^{\delta}$$

$$\left. + (k_1^2 - k_s^2) \int_{-\delta}^{\delta} \begin{pmatrix} \sin k_s z' \\ \cos k_s z' \end{pmatrix} \frac{e^{-jk_1 R}}{R} dz' \right\} \quad (5)$$

where $R = \sqrt{[\rho^2 + (z - z')^2]}$. By successively using $\kappa_1 = h_1$ and $k_1 = h_2$ in the above equations, the electric fields of a current source in a chiral medium are added to obtain the total field. The terms involving $\omega \mathbf{x} \nabla$ in Eq. (1) have the form of the magnetic field of a current filament in an achiral medium, so their evaluation also can use the existing code. These terms are not needed for wire objects lying in a plane, however. Note that for an ordinary medium, k_s is set equal to the medium wavenumber k, so that the integrals in Eqs. (4) and (5) drop out.

The optimum choice for k_s in Eq. (3) is not as clear as for a wire in a chiral medium as in the achiral case. Experience with modeling wires in chiral media has shown [Bhattacharyya, Burke and Miller (1992a), Bhattacharyya, Burke and Miller (1992a)] that the current travels along the wire with a propagation constant approximately $\sqrt{(h_1 h_2)}$, but with somewhat smaller phase constant and increased attenuation. Hence, k_s is usually set equal to $\sqrt{(h_1 h_2)}$. The alternate value $k_s = \max(h_1, h_2)$ has also been used, and gives results very close to the former choice as long as $|k_s \Delta_i| \ll 1$ for all segments on the wires. This result shows that the solution can converge to the correct result independent of the choice of k_s so long as the basis function is able to accurately enough represent the actual current. In fact, Eq. (3) becomes approximately a quadratic function of s when $|k_s \Delta_i| \ll 1$.

Results for Wire Antennas in Chiral Media

The chiral version of NEC (CHNEC), based on the analytical and numerical treatment discussed above, has been tested for problems involving an infinite chiral medium as well as for a vertical dipole located near a chiral half space, a problem discussed elsewhere [Bhattacharyya, Burke and Miller (1992b)]. Results obtained from CHNEC have been checked in various ways, some of which are reported here. The radiation resistance of a short dipole antenna in an infinite chiral medium was found to be in good agreement with the result in taking into account that a constant current is assumed in the latter while the CHNEC solution yields a natural triangular current distribution. The current on a $6\lambda_0$ dipole is shown in Fig. 1, and is close to that presented by Jaggard et. al. (1991) except for an unexplained difference in the current magnitude. As separate checks, for both the short dipole and the $6\lambda_0$ dipole, the total radiated power as obtained by integrating the radiated field from CHNEC was found agreed to within 1 percent of the computed input power. Note that reference here to object size in wavelengths is with respect to the achiral-medium situation, i.e., when $\gamma = 0$.

The current magnitude on a 30-wavelength long wire is plotted in Fig. 2 for chirality $\gamma = 0.01$ with the wire radius "a" a parameter. The wire is excited one-quarter wavelength from the left end and is resistively loaded at the right to reduce end reflections. As wire radius increases, we note an increased attenuation of the current. This behavior is observed in achiral media as an increase in the radiation resistance of a dipole with increasing radius. In this case, however, we observe two different attenuation regions. One begins at the feedpoint and is a region of higher attenuation the value of which seems to be dependent on wire radius. The other region is seen further out when the current has decayed adequately and where lower attenuation occurs, the value of which seems to be independent of wire radius. It is apparent that there is a change in the propagation characteristic of the current between these two regimes.

This is made more apparent in Fig. 3 by plotting both he magnitude and phase of the current for a $= 10^{-4}\lambda_0$. There we see that the wavelength associated with the high-attenuation rate is much shorter than that for the low-attenuation rate. In each region, the wavelength is longer than λ_0, indicating that both are what is called a "fastwave" region. Further evidence for the fastwave near-source current is provided in Fig. 4 where the attenuation ($-\alpha$) and phase ($\pm j\beta$) constants are plotted versus chirality for two different values of wire radius for the near-source current as obtained from estimating the wavenumber from the current on a $6\lambda_0$ wire. The CHNEC results are found to agree well with those obtained from evaluating the pole in the current spectrum of an infinite cylindrical antenna [Bhattacharyya, Burke and Miller (1992c)].

The input impedance of a center-fed dipole is shown as a function of chirality for a medium having $\epsilon_r = 2.56$ and $\mu_r = 1.0$ for lengths of 0.5λ and 1.0λ in Fig. 5. The half-wave dipole is "tuned" through resonance, a phenomenon also produced for the full-wave dipole at a slightly greater value of chirality. These results seem to indicate the possibility of tuning antennas embedded in chiral media or possibly plated on chiral substrates if the chirality can be controlled.

Our concluding results in Fig. 6 are for the input impedance of a loop antenna in a medium having $\epsilon_r = 2.56$ and $\mu_r = 1.0$ as a function of chirality for antenna circumferences of 0.5λ, 1.0λ, 1.6λ, and 5.03λ. In each case, the changing chirality produces oscillations in the input impedance, but which cannot be accurately described as resonances at least in the sense that the reactance does not always change sign. For the loop as well, it appears as though ,were the chirality of the medium in which the antenna is embedded to be controllable, that some degree of control could be produced over its input impedance.

Concluding Comments

We have demonstrated extension of NEC, implemented in a model called CHNEC, to the problem of modeling wire objects located in infinite, chiral media. Although attention here was limited to simple dipoles and loops excited as antennas, CHNEC is now applicable to the same kinds of wire objects, e.g., non-planar wire configurations and wire mesh approximations to solid surfaces, as is NEC itself. Furthermore, work is underway to extend the present interface treatment in CHNEC, presently limited to vertical wires over a chiral halfspace, to the same kinds of halfspace problems as NEC now handles for achiral media. Validation of CHNEC has been accomplished by using power-conservation checks, wavenumber comparison with infinite-antenna solutions, and comparison with other chiral results. Having the general kind of modeling capability represented by CHNEC means that we are now able to explore how chirality might modify the characteristics of antennas and scatterers located in or near chiral media for various design purposes.

References

Bassiri, S., N. Engheta and C. H. Papas (1986), "Dyadic Green's Function and Dipole Radiation in Chiral Medium," *Alta Frequenza*, **LV**, 2, pp. 83-88.

Bassiri, S. (1990), "Electromagnetic Waves in Chiral Medium," in *Recent Advances in Electromagnetic Theory*, H. N. Kritikos and D. L. Jaggard, Ed., Springer-Verlag.

Bhattacharyya, A. K. (1990),"Control of Radar Cross Section and Cross-Polarization Characteristics of an Isotropic Chiral Sphere," *Electronics Letters*, **26**, 14, pp. 1066-1067.

Bhattacharyya, A. K., G. J. Burke, and E. K. Miller (1992a), "Circular Loop antenna In Unbounded Chiral Medium: A Moment-Method Solution," Accepted for publication in *Journal of Electromagnetic Waves and Applications*.

Bhattacharyya, A. K., G. J. Burke, and E. K. Miller (1992b),"Modeling Wire Dipoles in An Infinite Chiral Medium and Vertically-Oriented Near a Chiral half space," *Microwave and Optical Technology Letters*, accepted for publication.

Bhattacharyya, A. K., G. J. Burke, and E. K. Miller (1992c), "Wavenumbers for Currents on Infinite- and Finite-Length Wires in a Chiral Medium," submitted to 1992 AP-S International Symposium, Chicago.

Burke, G. J. and A. J. Poggio (1981), "Numerical Electromagnetic Code (NEC)--Method of Moments," Lawrence Livermore Laboratory Rept. UCID-18834, January.

Engheta, N., P. Pelet and G. Li (1991), "Edge Diffraction in Chiral Medium and RCS Applications: Meixner Edge Condition and the Sommerfeld Half-Plane Problem in Chiral Medium," *IEEE/URSI Meeting*, Session 24, U. of Western Ontario, London, Ontario, Canada.

Jaggard, D. L, J. C. Lin, A. C. Grot and P. Pelet (1991), "Thin Wire Antennas in Chiral Medium," *Electronics Letters*, **27**, 3, pp. 243-244.

Lakhtakia, A., V. K. Varadan and V. V. Varadan (1986), "A Parametric Study of Microwave Reflection Characteristics of a Planar Achiral-Chiral Interface," *IEEE Trans. Electromag. Compat.*, **EMC-28**, 2, pp.

Lakhtakia, A., V. K. Varadan and V. V. Varadan (1989). "Time-Harmonic Fields in Chiral Medium," *Springer-Verlag*.

Lakhtakia, A. (1990), ed., *Selected Papers in Optical Activity*, SPIE Milestone Series, SPIE Optical Eng. Press.

Lakhtakia, A., V. K Varadan and V. V. Varadan (1990), "Reflection of Plane Waves at Planar Achiral-Chiral Interface: Interdependence of the Reflected Polarization State," *J. Opt. Soc. Amer.*, **7**, 9, pp. 1654-1658.

Lakhtakia, A. (1991), "Recent Contribution to Classical Electromagnetic Theory of Chiral Materials: What Next?," *Speculat. Sci. Technol.*, **14**, 1, pp. 2-17.

Uslenghi, P. L. E. (1990), "Scattering by an Impedance Sphere Coated with a Chiral Layer," *Electromagnetics*, **10**, pp. 201-211.

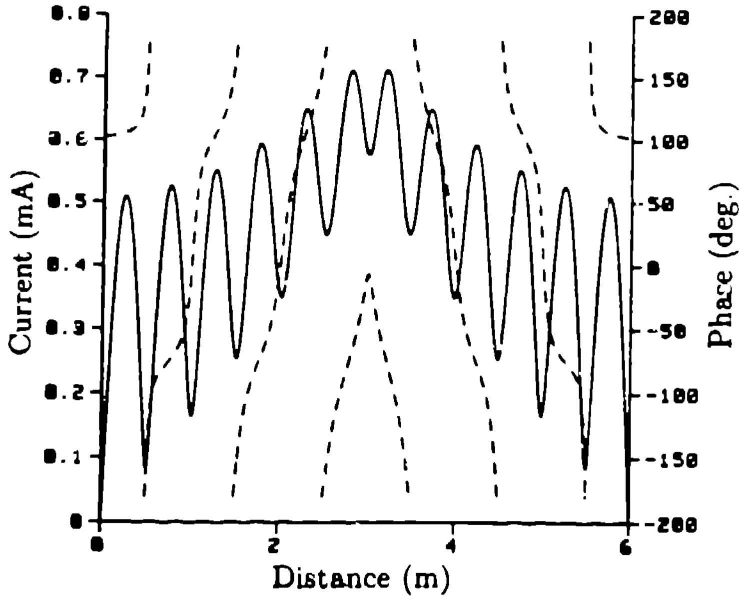

Fig. 1. Current on a dipole antenna of length $6\lambda_0$ and radius $10^{-6}\lambda_0$ in a chiral medium having $\varepsilon_r = \mu_r = 1.0$ and $\gamma\eta_0 = 1.0$, modeled using CHNEC and 121 segments. The current magnitude is shown as a solid line and the phase as a dashed line.

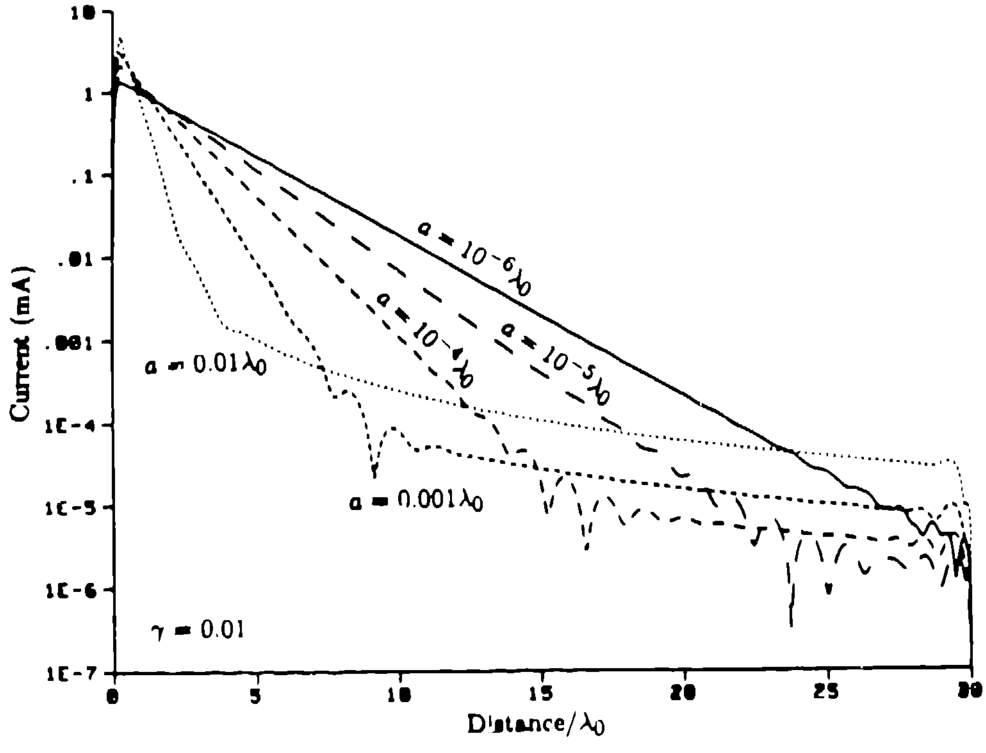

Fig. 2. Current magnitude on a $30\lambda_0$ wire with wire radius "a" a parameter for a chiality of $\gamma = 0.01$. The faster-decay slope that starts at the source may be seen to depend on wire radius, while the slower-decay region, when it is present, is apparently independent of radius.

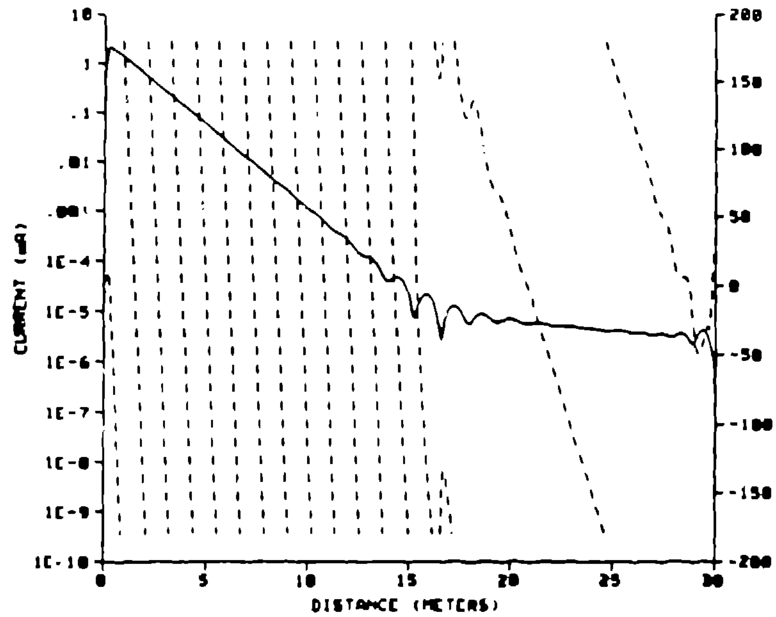

Fig. 3. The current magnitude (solid line) and phase (dashed line) on a $30\lambda_0$ wire for a chirality $\gamma = 0.01$ and a wire radius of $a = 10^{-4}\lambda_0$. The effective wavelength, as measured by the current phase progression with distance, can be seen to change from a value somewhat longer than λ_0 to one much longer than λ_0 at about the wire midpoint. The distance of this transition region depends on the wire radius, as seen in Fig. 2.

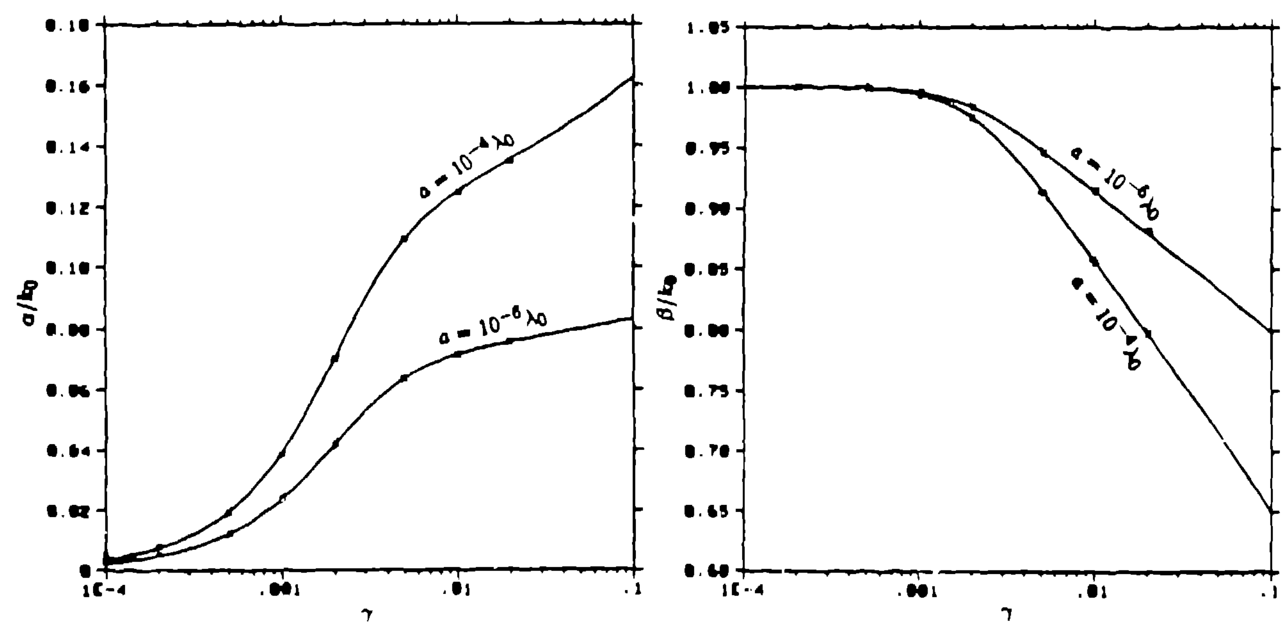

Fig. 4. The attenuation ($-\alpha$) and phase ($\pm j\beta$) constants on a wire as determined from the poles in the infinite antenna current spectrum (the solid line) and as estimated from CHNEC for a $6\lambda_0$ wire are shown as a function of chirality. The good agreement between these two results provides mutual validation for both. Note that these propagation constants apply to the near-source region of Figs. 2 and 3.

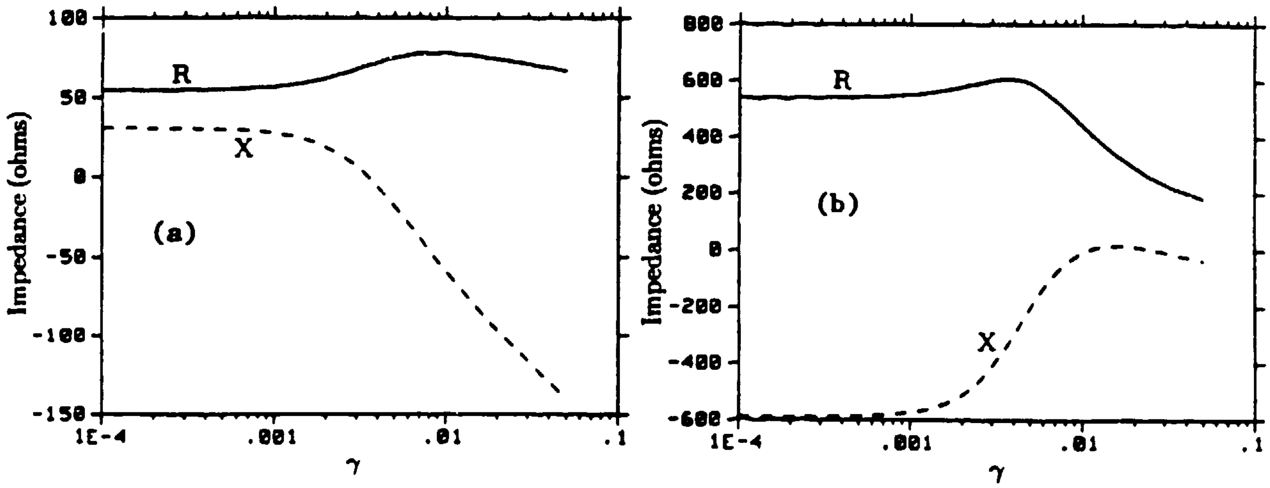

Fig. 5. The input impedance of a center-fed dipole $0.5\lambda_0$ (a) and $1.0\lambda_0$ (b) in length as a function of chirality. Chirality can evidently be used to "tune" a dipole through resonance.

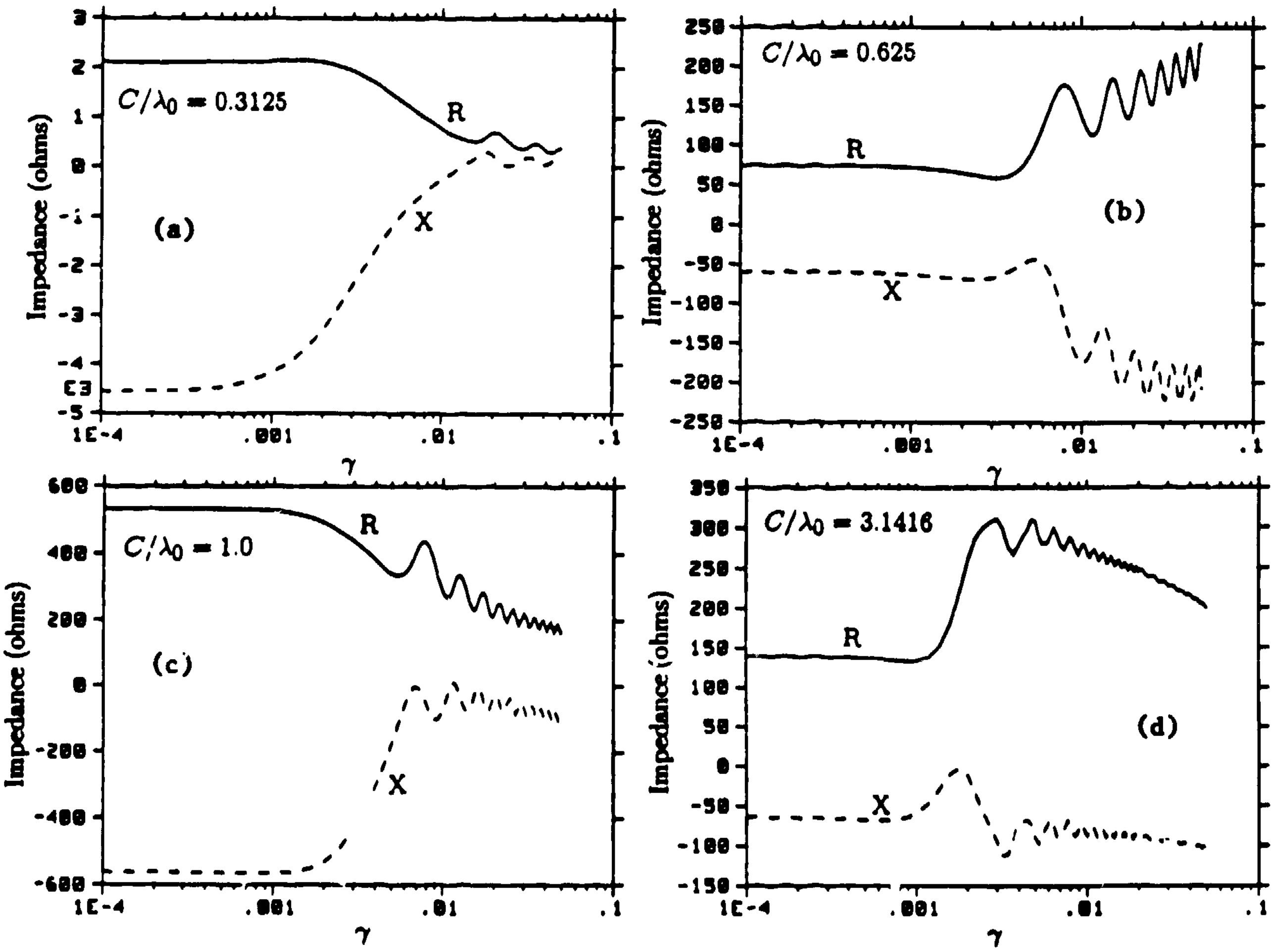

Fig. 6. The input impedance of a loop antenna of circumference $0.3128\lambda_0$ (a), $0.625\lambda_0$ (b), $1.0\lambda_0$ (c), and $3.1416\lambda_0$ (d) as a function of chirality for $\epsilon_r = 2.56$ and $\mu_r = 1.0$. A marked change in impedance occurs for γ increasing from 0.01 to 0.1.